Multiple Sclerosis and Related Disorders 79 (2023) 104991

Contents lists available at ScienceDirect

Multiple Sclerosis and Related Disorders

journal homepage: www.elsevier.com/locate/msard

Original article

Smoking affects epigenetic ageing of lung bronchoalveolar lavage cells in Multiple Sclerosis

Dennis Klose [a], Maria Needhamsen [a], Mikael V. Ringh [a], Michael Hagemann-Jensen [b], Maja Jagodic [a], Lara Kular [a,*]

[a] Department of Clinical Neuroscience, Karolinska Institutet, Center for Molecular Medicine, Karolinska University Hospital, 171 76 Stockholm, Sweden
[b] Department of Medicine, Solna, Karolinska Institutet, 171 76 Stockholm, Sweden

ARTICLE INFO

Keywords:
Multiple Sclerosis
Lung alveolar macrophages
Smoking
Ageing
Epigenetic clocks
DNA methylation
Inflammation

ABSTRACT

Background: A compelling body of evidence implicates cigarette smoking and lung inflammation in Multiple Sclerosis (MS) susceptibility and progression. Previous studies have reported epigenetic age (DNAm age) acceleration in blood immune cells and in glial cells of people with MS (pwMS) compared to healthy controls (HC).
Objectives: We aimed to examine biological ageing in lung immune cells in the context of MS and smoking.
Methods: We analyzed age acceleration residuals in lung bronchoalveolar lavage (BAL) cells, constituted of mainly alveolar macrophages, from 17 pwMS and 22 HC in relation to smoking using eight DNA methylation-based clocks, namely AltumAge, Horvath, GrimAge, PhenoAge, Zhang, SkinBlood, Hannum, Monocyte clock as well as two RNA-based clocks, which capture different aspects of biological ageing.
Results: After adjustment for covariates, five epigenetic clocks showed significant differences between the groups. Four of them, Horvath ($P_{adj} = 0.028$), GrimAge ($P_{adj} = 4.28 \times 10^{-7}$), SkinBlood ($P_{adj} = 0.001$) and Zhang ($P_{adj} = 0.02$), uncovered the sole effect of smoking on ageing estimates, irrespective of the clinical group. The Horvath, SkinBlood and Zhang clocks showed a negative impact of smoking while GrimAge detected smoking-associated age acceleration in BAL cells. On the contrary, the AltumAge clock revealed differences between pwMS and HC and indicated that, in the absence of smoking, BAL cells of pwMS were epigenetically 5.4 years older compared to HC ($P_{adj} = 0.028$). Smoking further affected epigenetic ageing in BAL cells of pwMS specifically as non-smoking pwMS exhibited a 10.2-year AltumAge acceleration compared to pwMS smokers ($P_{adj} = 0.0049$). Of note, blood-derived monocytes did not show any MS-specific or smoking-related AltumAge differences. The difference between BAL cells of pwMS smokers and non-smokers was attributable to the differential methylation of 114 AltumAge-CpGs ($P_{adj} < 0.05$) affecting genes involved in innate immune processes such as cytokine production, defense response and cell motility. These changes functionally translated into transcriptional differences in BAL cells between pwMS smokers and non-smokers.
Conclusions: BAL cells of pwMS display inflammation-related and smoking-dependent changes associated to epigenetic ageing captured by the AltumAge clock. Future studies examining potential confounders, such as the distribution of distinct BAL myeloid cell types in pwMS compared to control individuals in relation to smoking may clarify the varying performance and DNAm age estimations among epigenetic clocks.

1. Introduction

Multiple sclerosis (MS), a leading cause of non-traumatic neurological disability among young adults, is an inflammatory demyelinating and neurodegenerative disease of the central nervous system (CNS) primarily affecting women (Filippi et al., 2018). Even though the exact cause of MS remains elusive, smoking stands among the strongest non-genetic risk factors for the development of MS (Hedström et al., 2011; Olsson et al., 2017). The effect of smoke exposure on immune cells is mediated, at least in part, by epigenetic mechanisms such as DNA methylation (DNAm), as demonstrated in blood immune cells (Marabita et al., 2017). Overall, epigenetic alterations detected in immune and CNS cells have been suggested to play a role in the processes underlying MS development and progression (Ewing et al., 2019; Kular et al., 2018,

* Corresponding author.
E-mail address: lara.kular@ki.se (L. Kular).

https://doi.org/10.1016/j.msard.2023.104991
Received 28 April 2023; Received in revised form 18 June 2023; Accepted 2 September 2023
Available online 9 September 2023

2019, 2022a).

Importantly, smoking has been associated with the risk to convert to progressive stage of MS (Graetz et al., 2019; Ramanujam et al., 2015). Moreover, compelling evidence suggest that the progression of disability is dependent on age-related processes (Scalfari et al., 2011; Confavreux and Vukusic, 2006; Tutuncu et al., 2013). Epigenetic clocks stand among the most reliable estimators of biological age and indicators of organismal health and lifespan than chronological age alone (Oblak et al., 2021; Horvath and Raj, 2018). We have previously reported accelerated epigenetic ageing, measured with DNAm-based age acceleration residuals (AARs), in peripheral blood immune cells and in post-mortem glial cells of people with MS (pwMS) (Kular et al., 2022b; Theodoropoulou et al., 2019). Interestingly, the age acceleration in blood immune cells has been shown to partly depend on the effect of smoking and to vary according to specific cell types (Theodoropoulou et al., 2019). Altogether, these findings imply that both inflammation and ageing and their interaction (Franceschi et al., 2000) are relevant in MS pathogenesis and are likely restricted to specific cell types and conditioned by environmental factors such as cigarette smoke.

The lung has been proposed as a site of immune cell priming prior to CNS infiltration (Odoardi et al., 2012; Glenn et al., 2019; Hosang et al., 2022). The putative contribution of a smoking-associated lung-brain axis is further reinforced by DNAm and gene expression changes observable in bronchoalveolar lavage (BAL) cells, which are enriched in $CD14^+$ alveolar macrophages, of pwMS both in the absence and presence of cigarette smoking (Ringh et al., 2021).

We here aimed to investigate the biological ageing in BAL cells of people with and without MS in relation to smoking. We exploited eight DNAm-based clocks, namely the novel deep-learning AltumAge clock (de Lima Camillo et al., 2022), Horvath clock (Horvath, 2013), GrimAge (Lu et al., 2019), PhenoAge (Levine et al., 2018), Zhang clock (Zhang et al., 2019), SkinBlood clock (Horvath et al., 2018), Hannum clock (Hannum et al., 2013), Monocyte clock (Liang et al., 2022) as well as two RNA-based clocks (Ren and Kuan, 2020; de Magalhães et al., 2009). Moreover, we assessed the impact of potential confounders on DNAm age estimation and further explored the biological meaning of the AAR differences in relation to tissue-specificity and transcriptional changes.

2. Methods

Details of methods (including statistics and R packages) are provided in Appendix Methods A.

2.1. Study samples and data

The cohort used in this study has been previously described (Ringh et al., 2021) and summarized in Table 1 and Appendix Table B1. BAL cells were collected from female individuals diagnosed with MS and healthy control donors. No change in lung functions measured as forced expiratory volume in 1 s (FEV1), forced vital capacity (FVC) and the resulting FEV1/FVC could be observed in MS patients compared to controls or in smokers compared to non-smokers (Ringh et al., 2021). The DNAm data, generated using the Illumina Infinium MethylationEPIC BeadChip and accessible under GSE151017 in the GEO database, and RNA-sequencing gene expression data were previously described (Ringh et al., 2021). We used two publicly available DNAm datasets from $CD14^+$ monocytes isolated from peripheral blood (Ewing et al., 2019; Kiselev et al., 2022), generated with the Illumina Infinium Methylation450K BeadChip and accessible under GSE189256, GSE43976 in the GEO database.

Table 1
Characteristics of the cohort used for DNAm age estimation.

	HC-NS	HC-S	MS-NS	MS-S
Samples (N)	12	10	8	9
Sex (F/M)	12/0	10/0	8/0	9/0
Age (m ± sd)	25 ± 4.7	31.3 ± 9.2	43.1 ± 11.3	35.1 ± 9
Self-reported packyears (m ± sd)	–	8.53 ± 6	–	16.6 ± 9.3
MS subtype (N)				
RRMS	–	–	6	9
SPMS	–	–	1	0
PPMS	–	–	1	0
EDSS (med ± iqr)	–	–	2.25 ± 2.5	2 ± 1
Disease duration (y ± sd)	–	–	4.9 ± 6.2	5.4 ± 4

N, number; F/M, female/male ratio; HC, healthy controls; MS, Multiple Sclerosis; RRMS, relapsing-remitting MS; SPMS, secondary progressive MS; PPMS, primary progressive MS; NS, non-smoker; S, smoker; m, mean; sd, standard deviation; EDSS, expanded disability status scale; med, median; iqr, interquartile range; y, years.

2.2. Methylation data processing and calculation of DNAm age

All analyses have been conducted with R (version 4.1.2) in the RStudio IDE (version 2021.09.01) if not stated otherwise. The mitotic cell division rate (epiTOC) was calculated using *getEpiTOC* function from the cgageR package (version 0.1.0). For Zhang age estimation we used the script provided under github.com/qzhang314/DNAm-based-age-predictor (elastic net regression model) and for monocyte age estimation we used the *agep* function (wateRmelon package version 2.0.0) with CpG probes and coefficients provided in the original publication (Liang et al., 2022). For AltumAge calculation, we used a script provided under github.com/rsinghlab/AltumAge (version 2022.1) with the Python language from the reticulate R package (version 1.26). Horvath age, PhenoAge, GrimAge, SkinBlood age, Hannum age, DNAm TL and DNAm PackYears were calculated using the Horvath online tool accessible under dnamage.genetics.ucla.edu. Availability of CpG sites before and after imputation are listed in Appendix Table B2 for each clock separately.

3. Results

3.1. The biological age estimation of BAL cells greatly varies between the clocks

We applied eight DNAm-based clocks, commonly used to estimate epigenetic and biological age, on a DNAm dataset of BAL immune cells, comprising 39 female donors, including 22 healthy controls (HC) and 17 pwMS (Ringh et al., 2021) (Table 1). The pan-tissue AltumAge and Horvath clocks capture systemic ageing processes, whereas the Zhang, Hannum and SkinBlood clocks capture blood and immune cell specific ageing processes. Since alveolar macrophages constitute the majority of BAL cells (Ringh et al., 2021), we also used a monocyte/macrophage-specific clock. Finally, PhenoAge and GrimAge capture biological ageing with GrimAge particularly focusing on the effects of smoking. Noteworthy, AltumAge differs from the seven other clocks as it is based on a deep learning rather than elastic net regression strategy.

As none of the eight clocks were specifically trained on BAL cells, we first addressed their overall performance in our dataset. Results are illustrated in Fig. 1 and summarized in Table 2. Specifically, we examined the overall alignment of estimated epigenetic ages to chronological ages (bisector), resulting in high R^2 values for optimal estimations, as well as potential age group-specific or systematic biases generally reflected by a high mean absolute error (MAE). Slight underestimation of younger and older individuals could be observed with AltumAge and Horvath clocks, respectively, whereas GrimAge/PhenoAge biological clocks showed systematic overestimation across the whole lifespan (Fig. 1). The Zhang clock achieved the highest R^2, with however a systematic overestimation of DNAm age resulting in the highest MAE of all tested clocks (Table 2). Overall, the SkinBlood clock presented with the best combination of high R^2 and low MAE values and the cell type

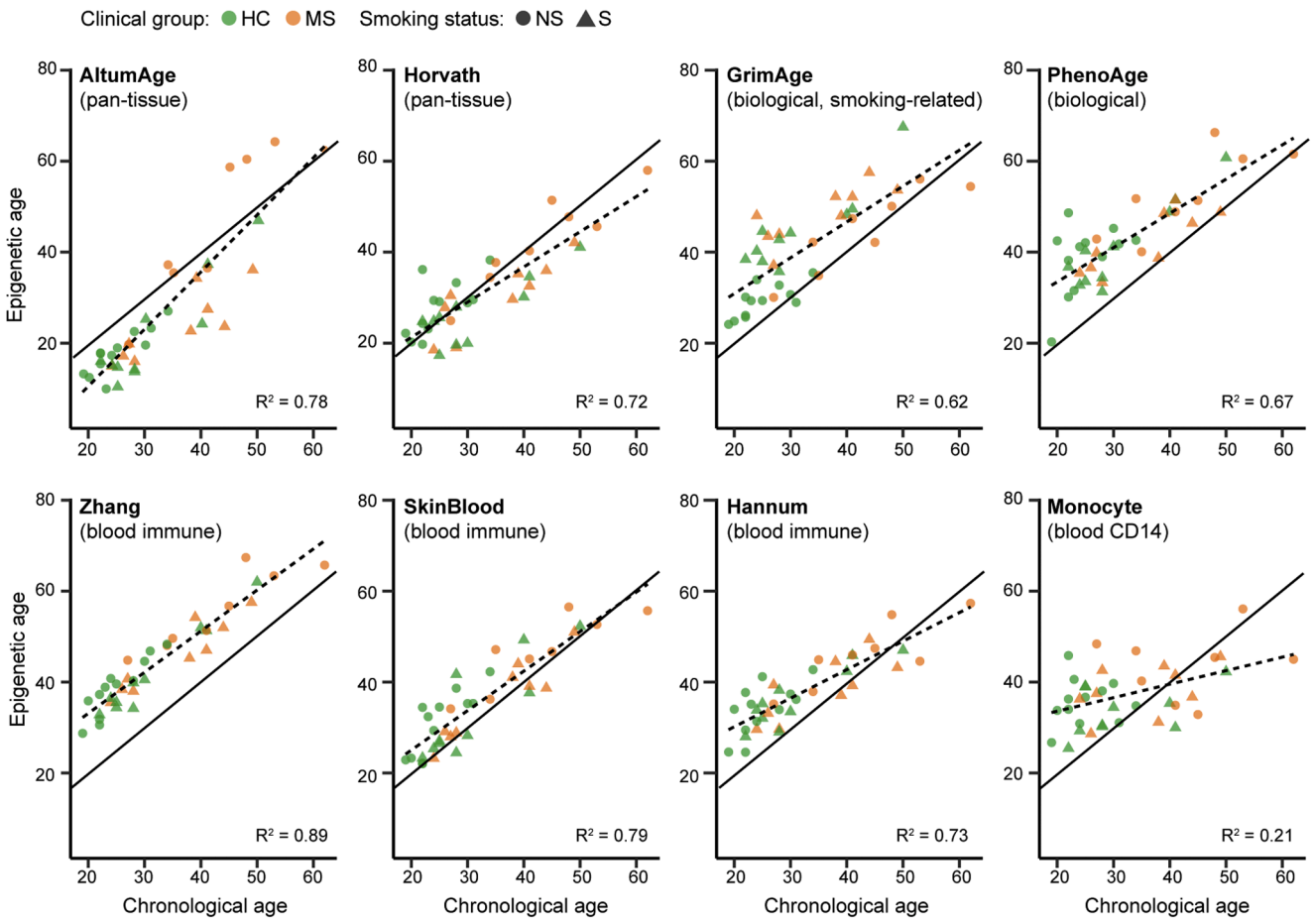

Fig. 1. Overview of DNAm age estimations by eight epigenetic clocks.
DNAm age estimations from AltumAge and Horvath (pan-tissue-based), GrimAge, PhenoAge, Zhang, Hannum and SkinBlood (whole blood-based) and Monocyte (monocyte-based) clocks. The black line represents the $x = y$ bisector and the dashed line represents the linear regression line of best fit. Legend: HC, healthy control; MS, Multiple Sclerosis; NS, non-smoker; S, smoker; R^2, Coefficient of determination.

Table 2
Quality metrics of age estimation by eight DNAm-based clocks and two RNA-based clocks.

	R^2	P	MAE
DNAm-based			
AltumAge	0.78	4.5×10^{-14}	8.4
Horvath	0.72	8.5×10^{-12}	4.6
GrimAge	0.62	2.3×10^{-9}	8.8
PhenoAge	0.67	1.4×10^{-10}	10.4
Zhang	0.89	1.2×10^{-19}	11.9
SkinBlood	0.79	3.5×10^{-14}	4.6
Hannum	0.73	2.9×10^{-12}	6.8
Monocyte	0.21	2.7×10^{-3}	8.7
RNA-based			
GTExAge	0.04	0.3	19.2
deMagalhães	0.0007	0.9	18.1

R^2, Coefficient of determination; P, P-Value; MAE, mean absolute error.

specific monocyte clock displayed the lowest correlation of DNAm and chronological age (Table 2, Fig. 1).

We tested the performance of transcriptomic (RNA-based) clocks in BAL cells of HC and pwMS (Appendix Table B1) using the GTExAge clock and the deMagalhães ageing signature (de Magalhães et al., 2009). We could confirm that estimation of biological age with transcriptomic data remains challenging and cannot compete with DNAm-based estimations. Indeed, both clocks yielded suboptimal R^2-values and displayed drastic deviations from the bisector, impeding proper interpretation of the estimated ageing residuals (Table 2, Appendix Fig. C1).

Thus, pan-tissue (AltumAge, Horvath) and blood-specific (Zhang, SkinBlood, Hannum) clocks outperform estimations from monocyte-specific and biological age (GrimAge, PhenoAge) clocks along with RNA-based clocks in our cohort of BAL cells.

3.2. *The pan-tissue clocks indicate significant AAR differences between sample groups in BAL cells*

We next analyzed epigenetic ageing in BAL cells in pwMS and HC stratified for smoking status, i.e. smokers (S) and non-smokers (NS), by calculating AARs, which overcomes estimation bias inherent to the clocks by regressing out the effect of chronological age on DNAm age. Out of eight clocks, the pan-tissue AltumAge and Horvath clock and the smoking-related biological GrimAge clock showed significant differences between AAR means across samples groups (Fig. 2). BAL cells of MS-NS displayed significantly higher AAR compared to MS-S with the AltumAge ($P < 0.001$) and Horvath ($P = 0.015$) clocks. Additionally, AltumAge resulted in higher AAR in MS-NS vs. HC-NS ($P = 0.049$), while the Horvath clock showed lower AAR in HC-S compared to HC-NS ($P = 0.005$). As expected, BAL cells of smoking HC and pwMS displayed significantly higher GrimAge AAR compared to non-smoking groups ($P < 0.0001$).

These findings underscore a noticeable variability in estimating epigenetic age, depending on which clock was used, with opposing estimations found between the smoking-related GrimAge clock and the

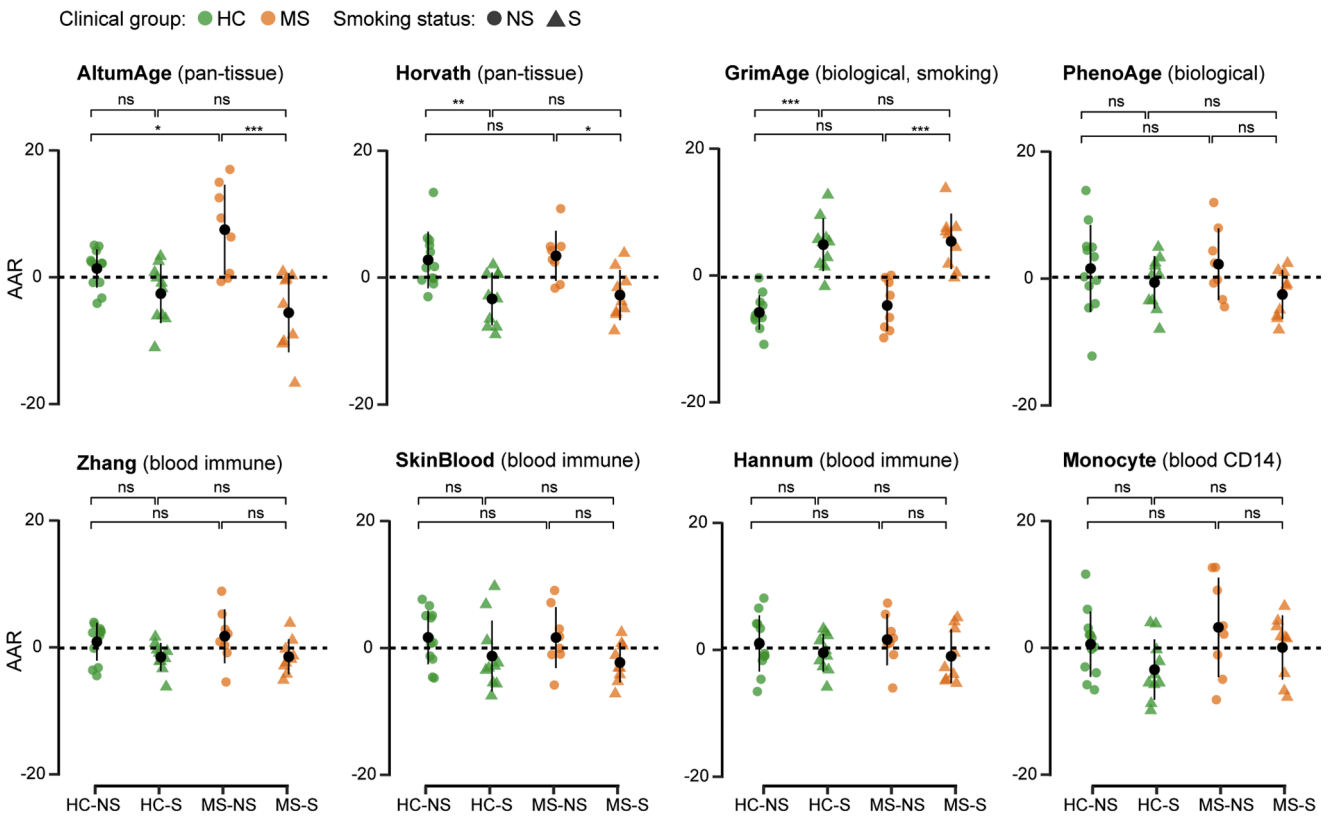

Fig. 2. Age acceleration residuals stratified for sample groups.
Significance was determined by Tukey HSD test (adjusted for multiple testing). Shown are sample means and standard deviations. Legend: HC, healthy control; MS, Multiple Sclerosis; NS, non-smoker; S, smoker. * $P < 0.05$, ** $P < 0.01$, *** $P < 0.001$, ns = not significant.

pan-tissue AltumAge/Horvath clocks.

3.3. *The AltumAge differences in BAL cells between sample groups are independent from tested confounders*

Given the discrepancies between the results of AltumAge/Horvath and GrimAge clocks, we investigated whether putative confounders might contribute to the results. We addressed the potential effect of cell type composition and smoking load (estimated by DNAm PackYears) as well as classical hallmarks of ageing including telomer length (TL) and mitotic division rate. We found significant correlations of AltumAge and Horvath AAR with all variables, except DNAm TL (Appendix Fig. C2). Investigation at the group level revealed significant differences in alveolar macrophage percentages ($P = 0.007$) and mitotic division rates ($P = 0.014$) between HC-S and HC-NS (Fig. 3(a) and (b)). The smoking load did not significantly differ between HC and MS smokers (Fig. 3(c)), ruling out a possible imbalance of smoke exposure. DNAm TL did not significantly differ across sample groups (Fig. 3(d)). Furthermore, we tested for the potential bias of self-reported smoking status using DNAm-based EpiSmoker categorization, which achieved 87% accuracy (overlap) in confirming self-reported smoking status ($P = 2.5 \times 10^{-6}$, Appendix Table B3). These findings jointly promoted us to include alveolar macrophage percentages and mitotic division rate as covariates in a MANCOVA model weighted for the probability of correctness of the self-

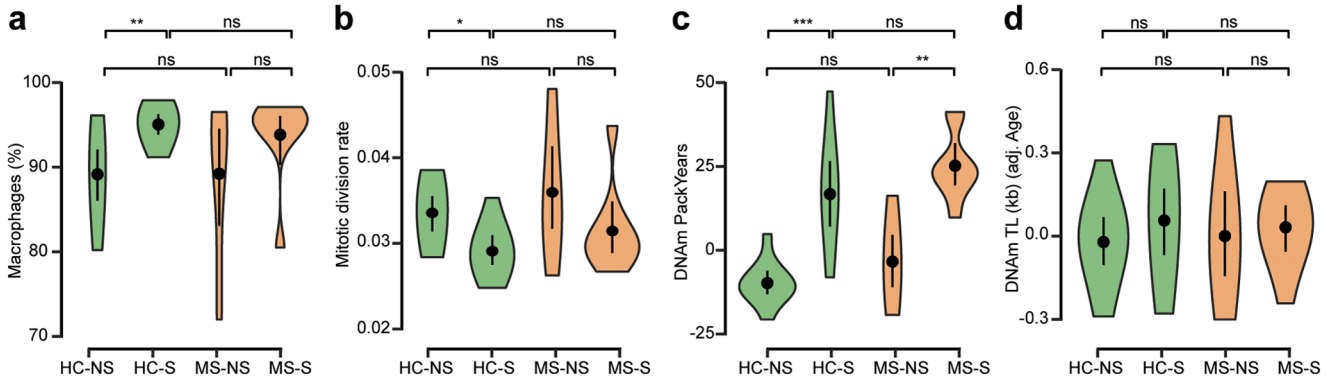

Fig. 3. Analysis of possible confounders per sample group.
a. Alveolar macrophage percentage as measured by FACS. b. DNAm mitotic division rate, with higher values indicating faster cell division. c. DNAm PackYears measure of smoking load. d. DNAm telomer length in kilobases adjusted for age. Shown are sample means and standard deviations. Colored area represents the distribution of each potential confounder. Legend: HC, healthy control; MS, Multiple Sclerosis; NS, non-smoker; S, smoker. * $P < 0.05$, ** $P < 0.01$, *** $P < 0.001$, ns = not significant. *P*-values are not adjusted for multiple testing.

reported smoking status. After adjustments, AltumAge estimated a significant 5.4-year AAR increase in BAL cells of MS-NS compared to HC-NS and a 9.5-year decrease in MS-S compared to HC-NS (Table 3). Outcomes of the Horvath clock uncovered the sole general effect of smoking, which exerted a significant DNAm age reduction of 6.1 years (Table 3). A general positive effect of smoking on GrimAge AAR remained significant using the same MANCOVA model ($P_{adj} = 4.28 \times 10^{-7}$, Table 3). Adjusting the five remaining epigenetic ageing measures for covariates revealed a significant negative effect of smoking on SkinBlood and Zhang AAR, independent of clinical group (Appendix Table B4).

Additionally, we explored the potential confounding effects of clinical features, including Expanded Disability Status Scale (EDSS), disease duration and medication, in the MS group for AltumAge. Unlike EDSS, disease duration was significantly associated to AltumAge AAR (Appendix Fig. C2). Medication did not significantly differ between MS smokers and non-smokers (Appendix Table B5). After adjustment for disease duration in pwMS with a separate MANCOVA model, the difference in AAR between MS-NS and MS-S remained significant ($P_{adj} = 0.0049$, Table 4). Of note, a residual negative effect of disease duration could be observed ($P = 0.038$, Table 4). Overall, at least 66% of variation in AltumAge AAR between MS non-smokers and smokers could be explained with the listed variables ($R^2 = 0.66$, $P = 0.0014$, Table 4).

Thus, the significantly accelerated epigenetic ageing observed in BAL cells of MS-NS in comparison to MS-S and HC-NS with the AltumAge clock withstands adjustment for covariates.

3.4. AltumAge clock captures ageing processes related to innate immune responses and cell motility in BAL cells of pwMS specifically

To reach an understanding of the ageing processes captured by the novel AltumAge clock, which relies on a neural network model including 20.318 CpG sites, we first compared AltumAge AAR with the AAR of the other clocks using a linear model. We found significant correlations of AltumAge AAR with Horvath clock and to a lesser extend to Zhang, Hannum and SkinBlood clocks, which jointly explained only 46% of AltumAge AAR variation (Appendix Table B6). We next asked whether the differences in AltumAge AAR were restricted to lung-confined BAL $CD14^+$ macrophages (Appendix Fig. C3) and calculated AltumAge AAR

Table 3
Adjusting AltumAge, Horvath and GrimAge AAR for potential confounders.

	Estimate	P_{adj}
AltumAge		
Intercept (HC:NS)	−0.16	0.99
MS	5.39	2.8×10^{-2}
S	−2.43	0.33
MS:S	−9.46	7.6×10^{-3}
Mitotic division rate	202.6	0.41
Alveolar macrophage %	−0.06	0.76
Adj. $R^2 = 0.43$, $P = 2.2 \times 10^{-4}$		
Horvath		
Intercept (HC:NS)	−5.1	0.78
MS	0.43	0.81
S	−6.1	3.8×10^{-3}
MS:S	−0.11	0.96
Mitotic division rate	237.6	0.22
Alveolar macrophage %	0.0002	0.99
Adj. $R^2 = 0.43$, $P = 2.1 \times 10^{-4}$		
GrimAge		
Intercept (HC:NS)	−9.37	0.52
MS	1.26	0.39
S	9.74	4.28×10^{-7}
MS:S	−0.89	0.67
Mitotic division rate	−280.7	0.07
Alveolar macrophage %	0.14	0.22
Adj. $R^2 = 0.78$, $P = 4.66 \times 10^{-11}$		

AAR, age acceleration residual; HC, healthy controls; MS, Multiple Sclerosis; NS, non-smoker; S, smoker; R^2, Coefficient of determination; *P*, *P*-Value; P_{adj}, adjusted *P*-Value; * $P < 0.05$, ** $P < 0.01$, *** $P < 0.001$.

Table 4
Adjusting AltumAge AAR for potential confounders for people with MS specifically.

	Estimate	P_{adj}	
Intercept (MS:NS)	−52.9	0.32	
MS:S	−10.2	0.0049	**
Disease duration	−0.73	0.038	*
Mitotic division rate	902	0.075	
Alveolar macrophage %	0.34	0.4	

Adj. $R^2 = 0.66$, $P = 1.4 \times 10^{-3}$

AAR, age acceleration residual; HC, healthy controls; MS, Multiple Sclerosis; NS, non-smoker; S, smoker; R^2, Coefficient of determination; *P*, *P*-Value; P_{adj}, adjusted *P*-Value; * $P < 0.05$, ** $P < 0.01$, *** $P < 0.001$.

in blood-derived $CD14^+$ monocytes from two publicly available datasets by Kiselev et al. (2022) (6 pwMS and 8 HC) and Ewing et al. (2019) (26 pwMS and 15 HC). AltumAge yielded reliable estimations of DNAm age across the lifespan (Appendix Fig. C4) but no difference in AAR means between HC and pwMS could be found, irrespective of adjustment for sex or stratification for EpiSmoker status (Appendix Fig. C4 and Table A7). This suggests the importance of lung localization of $CD14^+$ cells in the context of MS and smoking.

To further investigate the functional meaning of AltumAge AAR in BAL cells and AltumAge-based age acceleration in MS-NS, we sought out to identify the most variable AltumAge-CpGs between MS-S and MS-NS. We used a two-step approach by first applying *ComBat* transformation to the methylation levels of pwMS according to their smoking status, which successfully reduced the variance and the significant AAR difference between MS-S and MS-NS (Appendix Fig. C5). We next identified the CpGs responsible for this effect using a linear model that notably incorporates ComBat (before/after) and is stratified for the smoking status (see Appendix Methods A). A total of 114 CpGs presented with significant associations ($P_{adj} < 0.05$). Consistently, they also stood among the most differentially methylated AltumAge sites between MS-S and MS-NS (Appendix Table B8) and were therefore likely to be responsible for the observed AltumAge AAR difference between MS-S and MS-NS. This effect seemed to be specific for the MS group as a similar approach addressing the significant AltumAge AAR difference between MS-NS vs. HC-NS yielded only one CpG site after correction for multiple testing and was therefore not pursued. As expected from the AltumAge design, the vast majority of the CpGs (84%, 95/114) mapped to gene segments associated to gene promoters (TSS200, TSS1500, 5′UTR) (Appendix Table B9), suggesting a functional link to transcriptional changes.

We next performed gene ontology (GO) analysis of the 111 unique genes annotated by these 114 CpGs and found an enrichment of "*Biological Processes*" related to immune functions predominantly related to pathogen response, cell adhesion and cytokine production (Fig. 4(a), Appendix Table B10). Interestingly, the DNAm changes were accompanied by gene expression differences in BAL cells of MS-S ($n = 3$) vs. MS-NS ($n = 7$) (Appendix Table B1), implying a functional impact of DNAm at these AltumAge-CpGs in BAL cells of pwMS in the context of smoking (Fig. 4(b)). Most of them displayed hypermethylation and concomitant reduced expression in MS-S compared to MS-NS with 21 paired DNAm and expression changes being significant after multiple testing correction ($P_{adj} < 0.05$) (Fig. 4(b), Appendix Table B11). Ingenuity Pathway Analysis of these 111 genes suggested lower activity of "*Biological processes*" pertaining to cellular motility, myeloid cell functions and inflammatory processes in MS-S compared to MS-NS (Fig. 4(c), Appendix Table B10). Impaired innate immune reactions were reflected by lower activity of "*Pathways*" related to cytokine production, NOS/ROS signaling and phagosome formation and S100 protein family signaling. The few terms displaying an increased activity in MS-S compared to MS-NS were related to LXR/RXR activation and infection (Fig. 4(c), Appendix Table B10). Accordingly, the AltumAge-CpG genes form a biologically connected network (interaction enrichment $P = 6 \times 10^{-6}$) with 61 core genes presented in Fig. 4(d).

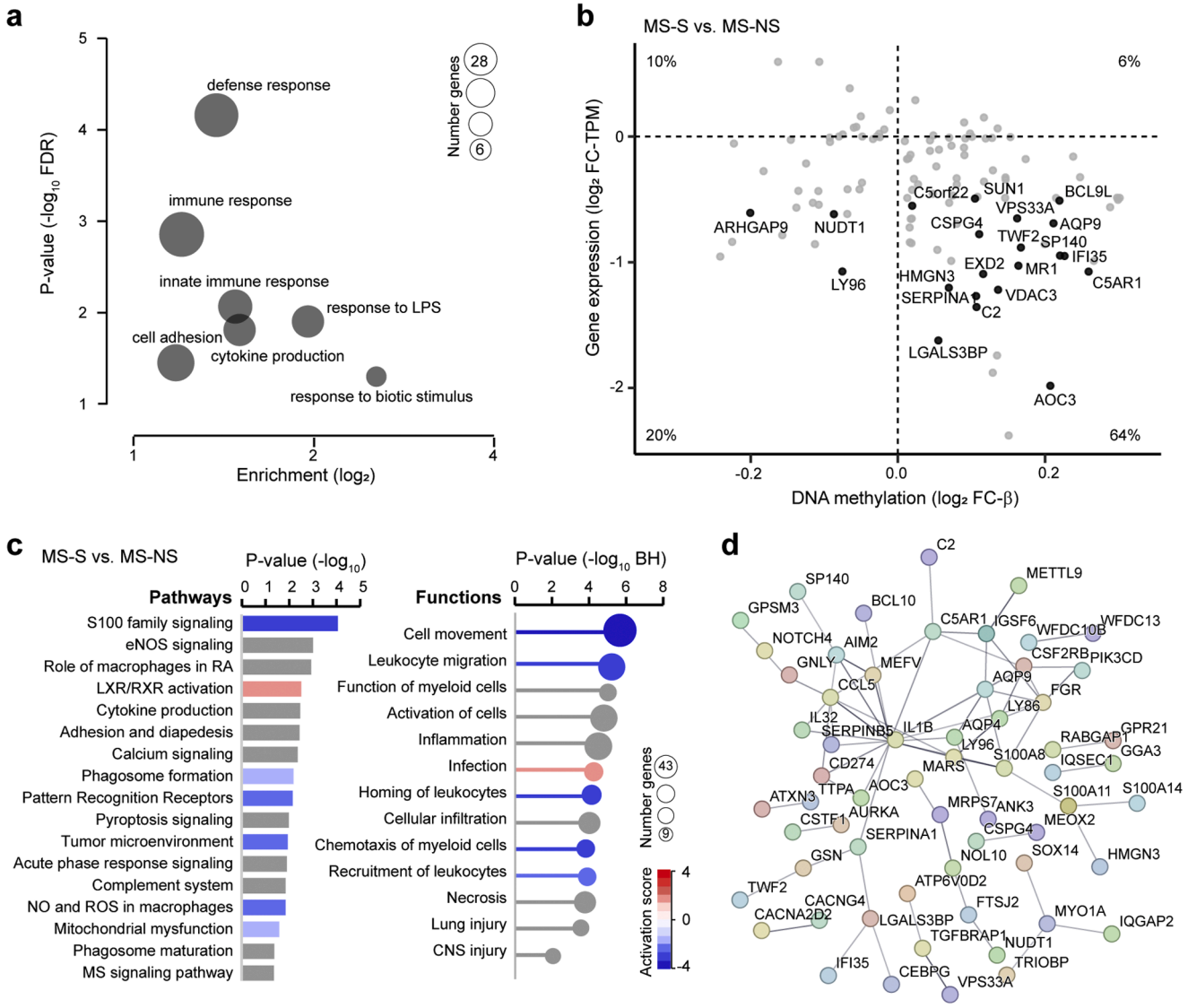

Fig. 4. AltumAge differences between MS smokers and non-smokers implicate innate immune processes related to cell motility and cytokine production.
(a) Gene ontology analysis, using overrepresentation analysis, of the genes annotated by the 114 CpG whose β-values significantly differed before and after ComBat transformation stratified for smoking status in our weighted limma model. The size of the circles reflects the number of genes included in each term. (b) Correlation between gene expression and DNAm fold changes of 114 β-values in MS-S compared to MS-NS. Percentage (%) of CpG-gene pairs is given for each quadrant. Black annotated circles indicate significant adjusted *P*-value for both fold changes. (c) *Pathways* analysis (left) and *Biological Functions and Diseases* (right), using Ingenuity Pathway analysis (IPA), of the genes annotated by the 114 AltumAge CpGs identified using Combat transformation. Blue to red color gradient represents low to high activation state of the term inferred by IPA according to transcriptional changes in MS-S compared to MS-NS. The size of the circles reflects the number of genes included in each term. (d) Representation of the core interconnected genes annotated by the 114 AltumAge CpGs using STRING network analysis. Grey gradient indicated the strength of data support (darker grey representing stronger evidence, i.e. combined interaction score >0.6). Legend: NS, non-smoker; S, smoker; MS, Multiple Sclerosis; AAR, age acceleration residual; FDR, false discovery rate; PC, principal component; TPM, transcripts per million; FC, fold change; ns, not significant; vs, versus.

Thus, a subset of 114 AltumAge-CpGs likely explains the age acceleration difference between BAL cells of MS-S and MS-NS. These DNAm changes primarily affected genes implicated in innate immune processes and cell motility and functionally translate into significant transcriptional differences.

4. Discussion

Despite well-established associations between cigarette smoking both with increased risk of developing MS (approximately 13% of cases of MS could be prevented by non-smoking (Manouchehrinia et al., 2022) and conversion to progressive disease (Hedström et al., 2011; Olsson et al., 2017; Graetz et al., 2019; Ramanujam et al., 2015) the underlying mechanisms remain elusive. We examined epigenetic and biological ageing of BAL cells in a case-control cohort and in relation to smoking. Our findings jointly support inflammation-related and smoking-dependent ageing in BAL cells of pwMS specifically.

Results from both pan-tissue clocks, AltumAge and Horvath, indicated slower epigenetic ageing in smokers compared to non-smokers, uncovering a surprising smoking-associated age deceleration. Likewise, a negative effect of smoking on AARs could be observed with the SkinBlood and Zhang clock, after adjustment for covariates. Smoking-induced age deceleration seems contradictory to the observed link between accelerated ageing and poor health outcomes in many tissues and further contrast with the outcome of the GrimAge clock, which is trained to capture the effect of smoking and consequently shows accelerated

ageing in BAL cells of smokers. On the other hand, age deceleration has been associated to more severe stages of Huntington's disease and poorer prognoses for certain types of cancer (Horvath et al., 2016; Ren et al., 2018; Lin and Wagner, 2015). A surprising DNAm age rejuvenation could also be observed in transplanted hematopoietic stem cells, independently of the donor's or recipient's age (Stölzel et al., 2017). Altogether, these findings emphasize the need for caution when interpreting DNAm age estimations as each clock seems to capture both common and distinct ageing-related molecular processes depending on the clinical context. Undoubtedly the limited size of the cohort, which is the main limitation of our study, might hinder the power to detect differences in the remaining ageing measures.

The most plausible factor that could influence the estimation of DNAm age and contribute to the smoking-related age deceleration in BAL cells is the presence of cellular heterogeneity in the myeloid cellular compartment. This might also explain the unexpected poor performance of the blood monocyte clock in BAL cells. Indeed, recent single-cell studies showed that the BAL milieu is populated by functionally distinct myeloid cell types, namely classical resident alveolar macrophages, non-classical monocyte-derived macrophages and blood monocytes recruited upon inflammation (Liégeois et al., 2022; De Man et al., 2023). Interestingly, the BAL composition is altered by smoking, which induces a concomitant increase of the number of stressed/damaged resident alveolar macrophages and recruited monocyte-derived macrophages, both cell subtypes exhibiting an activated and proinflammatory gene expression profile (Liégeois et al., 2022). Senescence also varies between monocyte-derived myeloid cells and resident alveolar macrophages, and some of the age-associated differentially expressed genes seem to be epigenetically regulated (De Man et al., 2023). Of note, the expression of *S100A8* gene included in the AltumAge clock appears specific to recruited macrophages, further supporting a link between varying cell types and DNAm age estimation. Accordingly, the AltumAge changes could not be detected in blood monocytes of pwMS and HC, highlighting the significance of the lung milieu in the context of MS, as previously evidenced in experimental models (Odoardi et al., 2012; Glenn et al., 2019; Hosang et al., 2022). Future studies examining the distribution of various BAL myeloid cell types in pwMS compared to control individuals in relation to smoking may clarify the impact of cellular heterogeneity on the DNAm age estimations. Moreover, even though AltumAge estimations were shown to be independent from obesity (de Lima Camillo et al., 2022), we were unable to address the potential effect of additional factors which might influence epigenetic ageing, such as depression, childhood socioeconomic status, BMI or alcohol consumption, due to the lack of available data in our cohort. Of note, while the use of an all-female cohort alleviates sex-dependent age estimations and is of high clinical relevance as MS primarily affects women, one cannot conclude with certainty that similar differences would have been observed in an all-male cohort.

While the negative effect of smoking on AAR was general with the Horvath, SkinBlood and Zhang clock and could not be replicated in each clinical group, the AltumAge clock revealed surprising MS-specific and smoking-dependent ageing dynamics characterized by accelerated ageing in BAL cell of non-smokers and age deceleration upon smoking. We could attribute this finding to methylation changes of a limited subset (0.005%) of promoter-associated AltumAge-CpGs in MS non-smokers compared to smokers, specifically. Interestingly, these changes appear functionally relevant as they translate into transcriptional dysregulation of the corresponding genes as well. Functional annotation further suggested that the smoking-related ageing changes in MS associate to an impairment of innate immune processes including cytokine production, phagocytosis, defense response and cell motility; such alterations have been previously reported in alveolar macrophages in the context of smoking in lung diseases (Lugg et al., 2022). The GO terms associated to defense response (e.g. LPS) are particularly interesting in light of the reported effect of lung microbiome changes (particularly towards LPS-producing phyla) on dampening MS-like disease symptoms in an animal model (Hosang et al., 2022). Of note, the difference between pwMS groups, which appears to be mainly driven by molecular changes in the MS non-smoker group, aligns with conclusions from our previous report showing molecular alterations of similar processes in BAL cells of non-smoker MS vs. HC, with eight AltumAge genes, *CD300E, AQP9, BCL9L, CAMKK1, FOLR3, SYT11, ATXN3, AQP9* and *ELOVL3*, overlapping with our previous study (Ringh et al., 2021). It is therefore tempting to speculate that the epigenetically older or younger pool of lung immune cells observed in our study may reflect a shift in cellular phenotype, pertaining to e.g. migratory capabilities found in the IPA analysis, which are linked to MS disease and smoking exposure. Thus, our findings confirm that BAL cells of pwMS exhibit a specific signature both in the absence and presence of smoking and further connect these inflammation-related changes to 'Altum ageing' processes. Additional studies in larger cohorts are warranted to disentangle the inflammation-specific from the ageing-dependent changes observed in BAL cells exposed to smoking.

5. Conclusions

In conclusion, our study provides novel insights into the inflammation- and smoking-related changes occurring in lung immune cells in people with MS and support age acceleration as a putative mechanism underlying MS disease. Given that cigarette smoking, which is often linked to symptoms of anxiety and depression experienced by pwMS (Vong et al., 2023), is the only modifiable factor that associates with MS severity, such knowledge has the potential to reinforce preventive and interventional measures towards a non-smoking lifestyle.

Statement of ethics

The study utilized publicly available data generated under the approval of the Regional Ethical Review Board in Stockholm (Reg. no. 2012/1782-31/1, 2012/1161-31/1) and methods were performed in accordance with institutional guidelines on human subject experiments. All subjects gave their written informed consent.

CRediT authorship contribution statement

Dennis Klose: Formal analysis, Investigation, Software, Visualization, Writing – original draft, Writing – review & editing. **Maria Needhamsen:** Supervision, Investigation. **Mikael V. Ringh:** Methodology. **Michael Hagemann-Jensen:** Methodology. **Maja Jagodic:** Supervision, Funding acquisition, Resources. **Lara Kular:** Conceptualization, Investigation, Supervision, Project administration, Funding acquisition, Data curation, Writing – original draft, Writing – review & editing.

Declaration of Competing Interest

Authors declare that they have no conflict of interest.

Funding

This study was supported by grants from the Swedish Research Council (No. 2021-02977, 2022-00650), the Swedish Association for Persons with Neurological Disabilities, the Swedish Brain Foundation, the Swedish MS Foundation, the Stockholm County Council - ALF project, the European Union's Horizon 2020 Research and Innovation Program (Grant agreement no. 733161) and the European Research Council (ERC) (Grant agreement no. 818170), the Knut and Alice Wallenberg Foundation, Åke Wilberg Foundation, Hedlund Foundation, Norlins Foundation, Bergvalls Foundation and Karolinska Institute's funds. LK is supported by a fellowship from the Margaretha af Ugglas Foundation. DK was supported by an Erasmus fellowship. The funders of the study had no role in study design, sample acquisition, data

collection, data analysis, data interpretation, or writing of the manuscript. We acknowledge support from the National Genomics Infrastructure in Stockholm funded by Science for Life Laboratory, the Knut and Alice Wallenberg Foundation and the Swedish Research Council (Grant agreement no. 2018-05973), and SNIC Multidisciplinary Center for Advanced Computational Science for assistance with massively parallel sequencing and access to the UPPMAX computational resources provided by Uppsala University..

Acknowledgments

We thank National Genomics Infrastructure (NGI), Science for Life Laboratory at Uppsala University, for processing methylation arrays, and the Uppsala Multidisciplinary Centre for Advanced Computational Science (UPPMAX; Uppsala University) for computational resources.

Supplementary materials

Supplementary material associated with this article can be found, in the online version, at doi:10.1016/j.msard.2023.104991.

References

Confavreux, C., Vukusic, S., 2006. Age at disability milestones in multiple sclerosis. Brain 129 (Pt 3), 595–605.
de Lima Camillo, L.P., Lapierre, L.R., Singh, R., 2022. A pan-tissue DNA-methylation epigenetic clock based on deep learning. npj Aging 8 (1), 4.
de Magalhães, J.P., Curado, J., Church, G.M., 2009. Meta-analysis of age-related gene expression profiles identifies common signatures of aging. Bioinformatics 25 (7), 875–881.
De Man, R., et al., *A multi-omic analysis of the human lung reveals distinct cell specific aging and senescence molecular programs.* bioRxiv, 2023.
Ewing, E., et al., 2019. Combining evidence from four immune cell types identifies DNA methylation patterns that implicate functionally distinct pathways during multiple sclerosis progression. EBioMedicine 43, 411–423.
Filippi, M., et al., 2018. Multiple sclerosis. Nat. Rev. Dis. Primers 4 (1), 43.
Franceschi, C., et al., 2000. Inflamm-aging. An evolutionary perspective on immunosenescence. Ann. N. Y. Acad. Sci. 908, 244–254.
Glenn, J.D., Liu, C., Whartenby, K.A., 2019. Frontline science: induction of experimental autoimmune encephalomyelitis mobilizes Th17-promoting myeloid derived suppressor cells to the lung. J. Leukoc. Biol. 105 (5), 829–841.
Graetz, C., et al., 2019. Association of smoking but not HLA-DRB1*15:01, APOE or body mass index with brain atrophy in early multiple sclerosis. Mult. Scler. 25 (5), 661–668.
Hannum, G., et al., 2013. Genome-wide methylation profiles reveal quantitative views of human aging rates. Mol. Cell 49 (2), 359–367.
Hedström, A.K., et al., 2011. Exposure to environmental tobacco smoke is associated with increased risk for multiple sclerosis. Mult. Scler. 17 (7), 788–793.
Horvath, S., 2013. DNA methylation age of human tissues and cell types. Genome Biol. 14 (10), R115.
Horvath, S., et al., 2016. Huntington's disease accelerates epigenetic aging of human brain and disrupts DNA methylation levels. Aging 8 (7), 1485–1512.
Horvath, S., et al., 2018. Epigenetic clock for skin and blood cells applied to Hutchinson Gilford progeria syndrome and ex vivo studies. Aging 10 (7), 1758–1775.
Horvath, S., Raj, K., 2018. DNA methylation-based biomarkers and the epigenetic clock theory of ageing. Nat. Rev. Genet. 19 (6), 371–384.
Hosang, L., et al., 2022. The lung microbiome regulates brain autoimmunity. Nature 603 (7899), 138–144.
Kiselev, I., et al., 2022. Genome-wide DNA methylation profiling identifies epigenetic changes in $CD4^+$ and $CD14^+$ cells of multiple sclerosis patients. Mult. Scler. Relat. Disord. 60, 103714.
Kular, L., et al., 2018. DNA methylation as a mediator of HLA-DRB1*15:01 and a protective variant in multiple sclerosis. Nat. Commun. 9 (1), 2397.
Kular, L., et al., 2019. Neuronal methylome reveals CREB-associated neuro-axonal impairment in multiple sclerosis. Clin. Epigenetics 11 (1), 86.
Kular, L., et al., 2022a. DNA methylation changes in glial cells of the normal-appearing white matter in multiple sclerosis patients. Epigenetics 17 (11), 1311–1330.
Kular, L., et al., 2022b. Epigenetic clock indicates accelerated aging in glial cells of progressive multiple sclerosis patients. Front. Aging Neurosci. 14, 926468.
Levine, M.E., et al., 2018. An epigenetic biomarker of aging for lifespan and healthspan. Aging 10 (4), 573–591.
Liang, X., et al., 2022. A new monocyte epigenetic clock reveals nonlinear effects of alcohol consumption on biological aging in three independent cohorts (N = 2242). Alcohol Clin. Exp. Res. 46 (5), 736–748.
Liégeois, M., et al., 2022. Airway macrophages encompass transcriptionally and functionally distinct subsets altered by smoking. Am. J. Respir. Cell Mol. Biol. 67 (2), 241–252.
Lin, Q., Wagner, W., 2015. Epigenetic aging signatures are coherently modified in cancer. PLoS Genet. 11 (6), e1005334.
Lu, A.T., et al., 2019. DNA methylation GrimAge strongly predicts lifespan and healthspan. Aging 11 (2), 303–327.
Lugg, S.T., et al., 2022. Cigarette smoke exposure and alveolar macrophages: mechanisms for lung disease. Thorax 77 (1), 94–101.
Manouchehrinia, A., et al., 2022. Smoking attributable risk in multiple sclerosis. Front. Immunol. 13, 840158.
Marabita, F., et al., 2017. Smoking induces DNA methylation changes in multiple sclerosis patients with exposure-response relationship. Sci. Rep. 7 (1), 14589.
Oblak, L., et al., 2021. A systematic review of biological, social and environmental factors associated with epigenetic clock acceleration. Ageing Res. Rev. 69, 101348.
Odoardi, F., et al., 2012. T cells become licensed in the lung to enter the central nervous system. Nature 488 (7413), 675–679.
Olsson, T., Barcellos, L.F., Alfredsson, L., 2017. Interactions between genetic, lifestyle and environmental risk factors for multiple sclerosis. Nat. Rev. Neurol. 13 (1), 25–36.
Ramanujam, R., et al., 2015. Effect of smoking cessation on multiple sclerosis prognosis. JAMA Neurol. 72 (10), 1117–1123.
Ren, J.T., et al., 2018. Decelerated DNA methylation age predicts poor prognosis of breast cancer. BMC Cancer 18 (1), 989.
Ren, X., Kuan, P.F., 2020. RNAAgeCalc: a multi-tissue transcriptional age calculator. PLoS One 15 (8), e0237006.
Ringh, M.V., et al., 2021. Methylome and transcriptome signature of bronchoalveolar cells from multiple sclerosis patients in relation to smoking. Mult. Scler. 27 (7), 1014–1026.
Scalfari, A., et al., 2011. Age and disability accumulation in multiple sclerosis. Neurology 77 (13), 1246–1252.
Stölzel, F., et al., 2017. Dynamics of epigenetic age following hematopoietic stem cell transplantation. Haematologica 102 (8), e321–e323.
Theodoropoulou, E., et al., 2019. Different epigenetic clocks reflect distinct pathophysiological features of multiple sclerosis. Epigenomics 11 (12), 1429–1439.
Tutuncu, M., et al., 2013. Onset of progressive phase is an age-dependent clinical milestone in multiple sclerosis. Mult. Scler. 19 (2), 188–198.
Vong, V., et al., 2023. The association between tobacco smoking and depression and anxiety in people with multiple sclerosis: a systematic review. Mult. Scler. Relat. Disord. 70, 104501.
Zhang, Q., et al., 2019. Improved precision of epigenetic clock estimates across tissues and its implication for biological ageing. Genome Med. 11 (1), 54.